Indian J. pure appl. Math., 33(8) : 1169-1182, August 2002
© Printed in India.

AXI-SYMMETRIC PROBLEM OF TIME HARMONIC SOURCES IN A MICROPOLAR ELASTIC MEDIUM

RAJNEESH KUMAR AND SUMAN CHOUDHARY

Department of Mathematics, Kurukshetra University, Kurukshetra 136 119, *Haryana*

(*Received* 26 *July* 2000; *after revision* 10 *July* 2001; *accepted* 5 *November* 2001)

A boundary-value problem corresponding to time harmonic vertical and horizontal loads acting in the interior of micropolar elastic medium is solved. The integral transforms have been inverted by using a numerical technique to obtain the normal displacement, normal force stress and tangential couple stress in the physical domain for different sources. The numerical results of these quantities for magnesium crystal like material are computed and illustrated graphically.

Key Words : Axi-Symmetric Problem; Harmonic Sources; Micropolar Elastic Medium

1. INTRODUCTION

Eringen and his coworker[3 & 12] developed a theory of simple microelastic solids in which the 'micro' deformations and 'micro' rotations of the material particles contained in a microvolume element with respect to its centroid are taken into account in an average sense. Materials affected by such micromotions and micro-deformations are called micro-morphic materials. Later on, Eringen[4] developed a theory for subclass of micro-morphic material which are called 'micropolar solids'. These solids represent the material that are made up of dipole atoms or dumbbell type molecules and are subjected to surface and body couples. The deformation in these materials is characterized not only by classical translation degrees of freedom represented by deformation vector field $\boldsymbol{u}(\boldsymbol{r}, t)$, but also by the rotation vector field $\boldsymbol{\phi}(\boldsymbol{r}, t)$.

Different authors have discussed different type of problems in micropolar elastic medium e.g., solution of the source problem for a finite three dimensional source in a micropolar elastic solid and disturbance in a micropolar elastic half-space due to axially symmetric source of finite length have been discussed by Sengupta and Ghosh[10 & 11], micropolar elastic fields due to a circular inclusion and micropolar elastic field due to spherical inclusion by Cheng and He[1 & 2]. Decay estimates for micropolar elastic cylinders by Nappa[8]. Tomar and Kumar[13] studied elastic wave propagation in a cylindrical bore situated in a micropolar elastic medium with stretch. Recently, Kumar and Deswal[6 & 7] discussed mechanical and thermal sources in a micropolar generalized thermoelastic medium and disturbance due to a point source in a generalized thermo-microstretch elastic medium.

Using the theory developed by Eringen[4], we study the disturbance due to a normal point source and tangential point source in the interior of a micropolar full-space by applying integral transform technique.

FORMULATION OF THE PROBLEM

We consider a uniform micropolar elastic medium of infinite extent with cylindrical co-ordinate system (r, θ, z). To analyze displacement and stresses at the interior of medium due to time harmonic concentrated load, the continuum is divided into two half-spaces defined by :

(*i*) half-space $I : 0 \le r < \infty, \ -\infty < z \le 0$

(*ii*) half-space $II : 0 \le r < \infty, \ 0 \le z < \infty$.

A time harmonic source is assumed to be acting on the interface of two half-spaces ($z = 0$) in the medium. We apply the arbitrary load $P(r, t) = P(r)\, e^{i\omega t}$.

Following Eringen[4], the constitutive relations and field equations in micropolar elastic solid without body force and body couple can be written as

$$t_{ij} = \lambda u_{k,k}\, \delta_{ij} + \mu (u_{i,j} + u_{j,i}) + K (u_{j,i} - \varepsilon_{ijk}\, \phi_k), \qquad \ldots (1)$$

$$m_{ij} = \alpha \phi_{k,k}\, \delta_{ij} + \beta \phi_{i,j} + \gamma \phi_{j,i}, \qquad \ldots (2)$$

$$(\lambda + \mu)\, \nabla (\nabla \cdot \boldsymbol{u}) + (\mu + K)\, \nabla^2 \boldsymbol{u} + K\, \nabla \times \boldsymbol{\phi} = \rho \frac{\partial^2 \boldsymbol{u}}{\partial t^2}, \qquad \ldots (3)$$

and

$$(\alpha + \beta + \gamma)\, \nabla (\nabla \cdot \boldsymbol{\phi}) - \gamma \nabla \times (\nabla \times \boldsymbol{\phi}) + K\, \nabla \times \boldsymbol{u} - 2K \boldsymbol{\phi} = \rho j \frac{\partial^2 \boldsymbol{\phi}}{\partial t^2}, \qquad \ldots (4)$$

where $\lambda, \mu, K, \alpha, \beta, \gamma$ are elastic constants, ρ is the density, j is the microinertia, $\boldsymbol{u}$ is the displacement vector, $\boldsymbol{\phi}$ is the microrotation vector, t_{ij} is the component of force stress tensor and m_{ij} is the component of couple stress tensor.

As we are considering axi-symmetric problem, so we take $\boldsymbol{u} = (u_r, 0, u_z)$ and $\boldsymbol{\phi} = (0, \phi_\theta, 0)$, with time harmonic behaviour as $\chi_i (r, z, t) = \chi_i (r, z)\, e^{i\omega t}$, $i = 1, 2, 3$,

where $\chi_1 = u_r, \chi_2 = u_z, \chi_3 = \phi_\theta$ and then define the non-dimensional quantities as

$$r' = \frac{r}{h}, \ z' = \frac{z}{h}, \ u_z' = \frac{u_z}{h}, \ u_r' = \frac{u_r}{h}, \ u_z' = \frac{u_z}{h}, \ t'^2 = \frac{\mu}{\rho h^2} t^2$$

$$\phi_\theta' = \frac{\mu}{\rho j \omega^{*2}} \phi_\theta, \ t_{ij}' = \frac{t_{ij}}{\mu}, \ m_{ij}' = \frac{h}{\gamma} m_{ij}, \ \omega'^2 = \frac{\rho h^2}{\mu} \omega^2. \qquad \ldots (5)$$

where

$$\omega^{*2} = \frac{K}{\rho j}, \ c_1^2 = \frac{(\lambda + 2\mu + K)}{\rho}$$

and h is a parameter having dimension of length.

Due to axial symmetry about z-axis, the quantities are independent of θ. With these considerations, the system of eqs. (3) and (4) may be rewritten into the dimensionless form after suppressing the dashes as

$$\frac{\partial e}{\partial r}+a_1\left[\nabla^2-\frac{1}{r^2}\right]u_r-a_2\frac{\partial \phi_\theta}{\partial z}=a_3\,u_r, \qquad \ldots (6)$$

$$\frac{\partial e}{\partial z}+a_1\,\nabla^2 u_z+a_2\left[\frac{\partial \phi_\theta}{\partial r}+\frac{\phi_\theta}{r}\right]=a_3\,u_z, \qquad \ldots (7)$$

and

$$\left[\nabla^2-\frac{1}{r^2}\right]\phi_\theta+b_1\left[\frac{\partial u_r}{\partial z}-\frac{\partial u_z}{\partial r}\right]=b_2\,\phi_\theta, \qquad \ldots (8)$$

where

$$a_1=\frac{(\mu+K)}{(\lambda+\mu)},\ a_2=\frac{K^2}{(\lambda+\mu)\,\mu},\ a_3=\frac{-\mu\,\omega^2}{(\lambda+\mu)}$$

$$b_1=\frac{h^2\mu}{\gamma},\ b_2=\frac{(2Kh^2-j\,\mu\,\omega^2)}{\gamma}$$

and

$$e=\frac{1}{r}\frac{\partial (ru_{r)}}{\partial r}+\frac{\partial u_z}{\partial z},\ \nabla^2=\frac{\partial^2}{\partial r^2}+\frac{1}{r}\frac{\partial}{\partial z}+\frac{\partial^2}{\partial z^2}.$$

With the aid of expressions relating displacement components u_r, u_z to the potential functions ψ_1, ψ_2 and microrotation vector ϕ_θ to the potential function Γ in dimensionless form given by,

$$u_r=\frac{\partial \psi_1}{\partial r}+\frac{\partial^2 \psi_2}{\partial r\,\partial z},\ u_z=\frac{\partial \psi_1}{\partial z}-\left[\nabla^2-\frac{\partial^2}{\partial z^2}\right]\psi_2 \text{ and } \phi_\theta=-\frac{\partial \Gamma}{\partial r}. \qquad \ldots (9)$$

in eqs. (6), (7) and (8), we obtain

$$[\nabla^2-a_4]\,\psi_1=0, \qquad \ldots (10)$$

$$[a_1\,\nabla^2-a_3]\,\psi_2+a_2\,\Gamma=0, \qquad \ldots (11)$$

and

$$[\nabla^2-b_2]\,\Gamma-b_1\,\nabla^2\,\psi_2=0, \qquad \ldots (12)$$

where

$$a_4=\frac{a_3}{1+a_1}.$$

Applying the Hankel transfors w.r.t. 'r' defined by

$$\{\hat{u}_z,\hat{\phi}_\theta\}\ (q,z,t)=\int_0^\infty \left\{u_z,\phi_\theta\right\}(r,z,t)\,rJ_0(rq)\,dr$$

and

$$\hat{u}_r(q,z,t)=\int_0^\infty u_r(r,z,t)\,r\,J_1(rq)\,dr \qquad \ldots (13)$$

to eqs. (10) and (12) and then eliminating $\hat{\Gamma}$ from the resulting expression, we obtain

$$\left[\frac{d^2}{dz^2} - m_2^2\right]\hat{\psi}_1 = 0, \qquad \ldots (14)$$

and

$$\left[\frac{d^4}{dz^4} + A\frac{d^2}{dz^2} + B\right]\hat{\psi}_2 = 0, \qquad \ldots (15)$$

where $m_2^2 = q^2 + a_4,\ A = a_5 - 2q^2,\ B = q^4 - a_5 q^2 + a_6,$

$$a_5 = \frac{b_1 a_2 - a_1 b_2 - a_3}{a_1} \text{ and } a_6 = \frac{a_3 b_2}{a_1}.$$

Since $\hat{\psi}_1$ and $\hat{\psi}_2$ tends to zero as z tends to infinity, the solution of eqs. (14) and (15) may be written as

$$\hat{\psi}_1 = A_1' e^{m_2 z} + A_1 e^{-m_2 z} \qquad \ldots (16)$$

and

$$\psi_2 = A_2' e^{\lambda_1 z} + A_2 e^{-\lambda_1 z} + A_3' e^{\lambda_2 z} + A_3 e^{-\lambda_2 z}, \qquad \ldots (17)$$

where

$$\lambda_{1,2}^2 = \left[\frac{-A \pm \sqrt{A^2 - 4B}}{2}\right],$$

where '+' sign corresponds to subscript '1' and '–' sign corresponds to subscript '2'.

Applying the Hankel transform defined by eq. (13) on eq. (12) and then using (17) in resulting expression, we get

$$\hat{T} = R_1 A_2' e^{\lambda_1 z} + R_1 A_2 e^{-\lambda_1 z} + R_2 A_3' e^{\lambda_2 z} + R_2 A_3 e^{-\lambda_2 z} \qquad \ldots (18)$$

where $R_i = E - F\lambda_i^2,\ (i = 1, 2)$

and

$$E = \frac{a_1 q^2 + a_3}{a_2},\ F = \frac{a_1}{a_2}.$$

Applying Hankel transform defined by eq. (13) on eq. (9) then using (16), (17) and (18) to evaluate $\hat{u}_r$ and $\hat{u}_z$ and $\hat{\phi}_\theta$ as

$$\hat{u}_r = -q\Big[A'_1 e^{m_2 z} + A_1 e^{-m_2 z} + \lambda_1 (A_2' e^{\lambda_1 z} - A_2 e^{-\lambda_1 z}) + \lambda_2 (A_3' e^{\lambda_2 z} - A_3 e^{-\lambda_2 z})\Big] e^{iwt}, \qquad \ldots (19)$$

$$\hat{u}_z = [m_2 (A_1' e^{m_2 z} - A_1 e^{-m_2 z}) + q^2 \left(A_2' e^{\lambda_1 z} + A_2 e^{-\lambda_1 z} + A_3' e^{\lambda_2 z} + A_3 e^{-\lambda_2 z}\right), \qquad \ldots (20)$$

and $$\hat{\phi}_\theta = q\left[R_1 A_2' e^{\lambda_1 z} + R_1 A_2 e^{-\lambda_1 z} + R_2 A_3' e^{\lambda_2 z} + R_2 A_3 e^{-\lambda_2 z} \right] e^{iwt}. \quad \ldots (21)$$

Making use of (5), (13) and (19)-(21) in eqs. (1) and (2), we obtain the stress components as

$$\hat{t}_{zz} = M_2 [A_1' e^{m_2 z} + A_1 e^{-m_2 z}] + S_1 [A_2' e^{\lambda_1 z} - A_2 e^{-\lambda_1 z}] + S_2 [A_3' e^{\lambda_2 z} - A_3 e^{-\lambda_2 z}], \quad \ldots (22)$$

$$\hat{t}_{zr} = M_1 [A_1' e^{m_2 z} - A_1 e^{-m_2 z}] + H_1 [A_2' e^{\lambda_1 z} + A_2 e^{-\lambda_1 z}] + H_2 [A_3' e^{\lambda_2 z} + A_3 e^{-\lambda_2 z}] \quad \ldots (23)$$

$$m_{z\theta} = N_1 [A_2' e^{\lambda_1 z} - A_2 e^{-\lambda_1 z}] + N_2 [A_3' e^{\lambda_2 z} - A_3 e^{-\lambda_2 z}], \quad \ldots (24)$$

where

$$M_1 = -qm_2 (K_1 + 1),\ M_2 = K_3 m_2^2 - K_4 q^2,$$

$$H_i = -(q K_1 \lambda_i^2 + q^3 + qK_2^2 R_i),\ (i = 1, 2),$$

$$S_i = (K_3 - K_4) q^2 \lambda_i,\ (i = 1, 2),\ N_i = qK_2 R_i \lambda_i,\ (i = 1, 2)$$

and $$K_1 = \frac{(\mu + K)}{\mu},\ K_2 = \frac{K}{\mu},\ K_3 = \frac{(\lambda + 2\mu + K)}{\mu} \text{ and } K_4 = \frac{\lambda}{\mu}.$$

The transformed displacements $\hat{u}_r^I$ and $\hat{u}_z^I$; microrotation $\hat{\phi}_\theta^I$; force stresses $\hat{t}_{zz}^I$ and $\hat{t}_{zr}^I$; and couple stress component $\hat{m}_{z\theta}^I$ for the region $-\infty < z \leq 0$ can be obtained by inserting following into eqs. (19)-(24);

$$A_1 = A_2 = A_3 = 0. \quad \ldots (25)$$

Similarly, $\hat{u}_r^{II}, \hat{u}_z^{II}, \hat{\phi}_\theta^{II}, \hat{t}_{zz}^{II}, \hat{t}_{zr}^{II}, \hat{m}_{z\theta}^{II}$ for the region $0 \leq z < \infty$ can be obtained by inserting following into eqs. (19)-(24);

$$A_1' = A_2' = A_3' = 0 \quad \ldots (26)$$

APPLICATION

Case I Load in Normal Direction

The boundary conditions for a load $P(r, t)$ applied at the interface $z = 0$ of two half-spaces in normal direction are

$$u_r^I(r, 0) - u_r^{II}(r, 0) = 0,\ u_z^I(r, 0) - u_z^{II}(r, 0) = 0,$$

$$\phi_\theta^I(r,0)-\phi_\theta^{II}(r,0)=0,\ m_{z\theta}^I(r,0)-m_{z\theta}^{II}(r,0)=0,$$

$$t_{zr}^I(r,0)-t_{zr}^{II}(r,0)=0,\ t_{zz}^I(r,0)-t_{zz}^{II}(r,0)=-P(r,t). \quad \ldots (27)$$

Case II Load in Radial Direction

The boundary conditions for a load $P(r, t)$ applied at the interface $z = 0$ of two half-spaces in the radial direction are

$$u_r^I(r,0)-u_r^{II}(r,0)=0,\ u_z^I(r,0)-u_z^{II}(r,0)=0,$$

$$\phi_\theta^I(r,0)-\phi_\theta^{II}(r,0)=0,\ m_{z\theta}^I(r,0)-m_{z\theta}^{II}(r,0)=0,$$

$$t_{zr}^I(r,0)-t_{zr}^{II}(r,0)=-P(r,t),\ t_{zz}^I(r,0)-t_{zz}^{II}(r,0)=0. \quad \ldots (28)$$

In order to determine the displacement and stress functions due to a concentrated load described as a Dirac Delta $\frac{\rho_0\delta(r)}{2\pi r}$, its Hankel transform with respect to the pair (r, q), defined by

$$\hat{p}(q)=\frac{\rho_0}{2\pi} \quad \ldots (29)$$

must be used. The final function in the (r, z) domain is obtained by a numerical inversion of the Hankel integral transform.

Case I load in normal direction

Making use of eqs. (20), (22), (24) and (29) in boundary conditions (27), we obtain the expressions for normal displacement, normal force stress, microrotation component and tangential couple stress as

$$\hat{u}_z=[m_2(\Delta_1 e^{m_2 z}-\Delta_2 e^{-m_2 z})+q^2(\Delta_3 e^{\lambda_1 z}+\Delta_4 e^{-\lambda_1 z}$$

$$+\Delta_5 e^{\lambda_2 z}+\Delta_6 e^{-\lambda_2 z})]\,e^{iwt}/\Delta, \quad \ldots (30)$$

$$\hat{t}_{zz}=[M_2(\Delta_1 e^{m_2 z}+\Delta_2 e^{-m_2 z})+S_1(\Delta_3 e^{\lambda_1 z}-\Delta_4 e^{-\lambda_1 z})$$

$$+S_2(\Delta_5 e^{\lambda_2 z}+\Delta_6 e^{-\lambda_2 z})]/\Delta, \quad \ldots (31)$$

$$\hat{\phi}_\theta=q\,[R_1(\Delta_3 e^{\lambda_1 z}+\Delta_4 e^{-\lambda_1 z})+R_2(\Delta_5 e^{\lambda_2 z}+\Delta_6 e^{-\lambda_2 z})]\,e^{iwt}/\Delta, \quad \ldots (32)$$

$$m_{z\theta}=[N_1(\Delta_3 e^{\lambda_1 z}-\Delta_4 e^{-\lambda_1 z})+N_2(\Delta_5 e^{\lambda_2 z}-\Delta_6 e^{-\lambda_2 z})]\,e^{iwt}/\Delta, \quad \ldots (33)$$

where $\Delta\ \rho=\rho_0/2\pi\ 8GG^*,\ \Delta_1=-\Delta_2=-4P(N_1\lambda_2-N_2\lambda_1)G,$

$$\Delta_3=\Delta_4=-4PN_2G,\ \Delta_5=\Delta_6=4PN_1G,$$

$$G = m_2 (R_2 H_1 - R_1 H_2) + q^2 M_1 (R_1 - R_2),$$

$$G^* = (N_2 S_1 - N_1 S_2) + M_2 (N_1 \lambda_2 - N_2 \lambda_1).$$

Particular Case — If we neglect the effect of micropolarity, that is, when $\alpha = \beta = \gamma = K = j = 0$, we obtain the expressions for displacement components and force stresses in the classical elastic medium as

$$\hat{u}_z = [m_2^* (\Delta_1^* e^{m_2^* z} - \Delta_2^* e^{-m_2^* z}) + q^2 (\Delta_3^* e^{\lambda_1^* z} + \Delta_4^* e^{-\lambda_1^* z})]/\Delta^*, \quad \ldots (34)$$

$$\hat{t}_{zz} = [M_2^* (\Delta_1^* e^{m_2^* z} + \Delta_2^* e^{-m_2^* z}) + S_1^* (\Delta_3^* e^{\lambda_1^* z} - \Delta_4^* e^{-\lambda_1^* z})]/\Delta^* \quad \ldots (35)$$

and $$\hat{t}_{zr} = M_1^* [\Delta_1^* e^{m_2^* z} - \Delta_2^* e^{-m_2^* z}] + H_1^* [\Delta_3^* e^{\lambda_1^* z} + \Delta_4^* e^{-\lambda_1^* z}]/\Delta^*, \quad \ldots (36)$$

where $$\Delta^* = 4 (\lambda_1^* M_2^* - S_1^*) (q^2 M_1^* - m_2^* H_1^*), \; \Delta_1^* = -\Delta_2^* = -2 \lambda_1^* P (q^2 M_1^* - m_2^* H_1^*),$$

$$\Delta_3^* = \Delta_4^* = 2P (q^2 M_1^* - m_2^* H_1^*),$$

$$M_1^* = -2qm_2^*, \; M_2^* = K_1^* m_2^{*2} - K_2^* q^2,$$

$$H_1^* = -(q^3 + q \lambda_1^{*2}), \; S_1 = (K_1^* - K_2^*) q^2 \lambda_1^*,$$

$$K_1^* = \frac{(\lambda + 2\mu)}{\mu}, \; K_2^* = \frac{\lambda}{\mu},$$

$$m_2^* = q^2 + a_3^*, \; \lambda_1^{*2} = q^2 + a_4^*,$$

and $$a_1^* = \frac{\mu}{(\mu + \lambda)}, \; a_2^* = -a_1^* \omega^2, \; a_3^* = \frac{a_2^*}{(1 + a_1^*)}, \; a_4^* = \frac{a_2^*}{a_1^*}.$$

Case II : Load in Radial Direction

Making use of (20), (22), (24) and (29) in the boundary conditions (28), we obtain the expressions of tangential couple stress, normal displacement and normal force stress as in eq. (30)-(32) with Δ_i replaced by Δ_i' (i = 1, 2, ..., 6) respectively where

$$\Delta_1' = \Delta_2' = 4q^2 P (R_2 - R_1) G^*, \; \Delta_3' = -\Delta_4' = -4m_2 R_2 PG^*,$$

$$\Delta_5 = -\Delta_6' = 4m_2 R_1 PG^*.$$

Particular Case

Neglecting the effect of micropolarity, the analytical expressions for displacement components and force stress are given by eqs. (34)-(36) with Δ_i^* replaced by $\Delta_i^{*'}$ (i = 1 2, 3, 4) respectively, where

$$\Delta_1^{*'} = \Delta_2^{*'} = -2q^2 P(\lambda_1^* M_2^* - S_1^*), \; \Delta_3^{*'} = -\Delta_4^{*'} = 2m_2^* P (\lambda_1^* M_2^* - S_1^*).$$

INVERSION OF TRANSFORM

We get expressions for displacement and stress component solution in eqns. (30)-(33) in the Hankel transform (q, z) domain. The final solution in the original domain (r, z) is obtained by a numerical inversion of the Hankel Integral transform.

These expressions are functions of z and the parameter of Hankel transform q and hence are of the form $\hat{f}(q, z)$. To get the function $f(r, z)$ in the Physical domain, we invert the Hankel transform using

$$f(r, z) = \int_0^\infty q \hat{f}(q, z) J_n(qr)\, dq \qquad \ldots (37)$$

The method for evaluating this integral is described in Press *et al.*[9], which involves the use of Romberg's integration with adaptive step size. This, also uses the results from successive refinements of the extended trapezoidal rule followed by extrapolation of the results to the limit when the step size tends to zero.

NUMERICAL DISCUSSION

In this section the numerical discussion for the time harmonic point source applied in the full space are reported. The analysis was conducted for Magnesium crystal like material. The values of elastic constants are taken as (Eringen[5])

$$\lambda = 9.4 \times 10^{11} \text{ dyne/cm}^2,\ \mu = 4 \times 10^{11} \text{ dyne/cm}^2,$$

$$K = 1 \times 10^{11} \text{ dyne/cm}^2,\ \rho = 1.74 \text{ gm/cm}^3,$$

$$\gamma = 0.779 \times 10^{-4} \text{ dyne},\ j = 0.2 \times 10^{-15} \text{ cm62}$$

The comparison of values of dimensionless normal displacement $U_z\,(= u_z/p)$, normal force stress $T_{zz}\,(= t_{zz}/P)$ and tangential couple stress $M_{z\theta}\,(= m_{z\theta}/p)$ for micropolar elastic solid (MES) and elastic solid (ES) have been studied and the variations of these components with distance 'r' have shown in Figs. 1, 2, 3, ..., 6. The computation were carried out for three values of dimensionless frequency ω = 0.80, 1.60 and 2.40 for $h^2 = 1 \times 10^{-15}\, cm^2$ at z = 1 in the range $0 < r \leq 10$. Solid line, either without centre symbols, [—] or with centre symbol [. .], corresponds to the case when ω = 0.80; small dashed line [---] or [-o - -o] corresponds to the case when ω = 1.60 and large dashed line [- - -] or [-o- -o -] to the case when ω = 2.40. For all the three frequencies solid lines or dashed lines without centre symbols represent the variations for MES, whereas lines with centre symbols for ES.

Case I Load in z-Direction

The variations of normal displacement, normal force stress and tangential couple stress with distance when normal point source is applied, have been shown in Figs. 1, 2, 3 respectively.

Fig. 1. shows the variations of normal displacement U_z with distance 'r' for three different frequencies. The values of U_z are more for MES than that for ES in the ranges $0 \le r \le 1.5$ and $2.5 \le r \le 4.5$ for all three frequencies. Initially, the value of U_z for ES increase sharply for all the three frequencies where as in *MES* it increase for $\omega = 0.8$ and decreased for $\omega = 1.6$ and ω 2.4. For *MES* the behavior of variations is oscillating in whole of the range whereas for *ES*, after a sharp increase in the value of U_z, it starts oscillating. The values of U_z, in the initial range, increase as frequency increases for *MES* but decreases as frequency increases for *ES*.

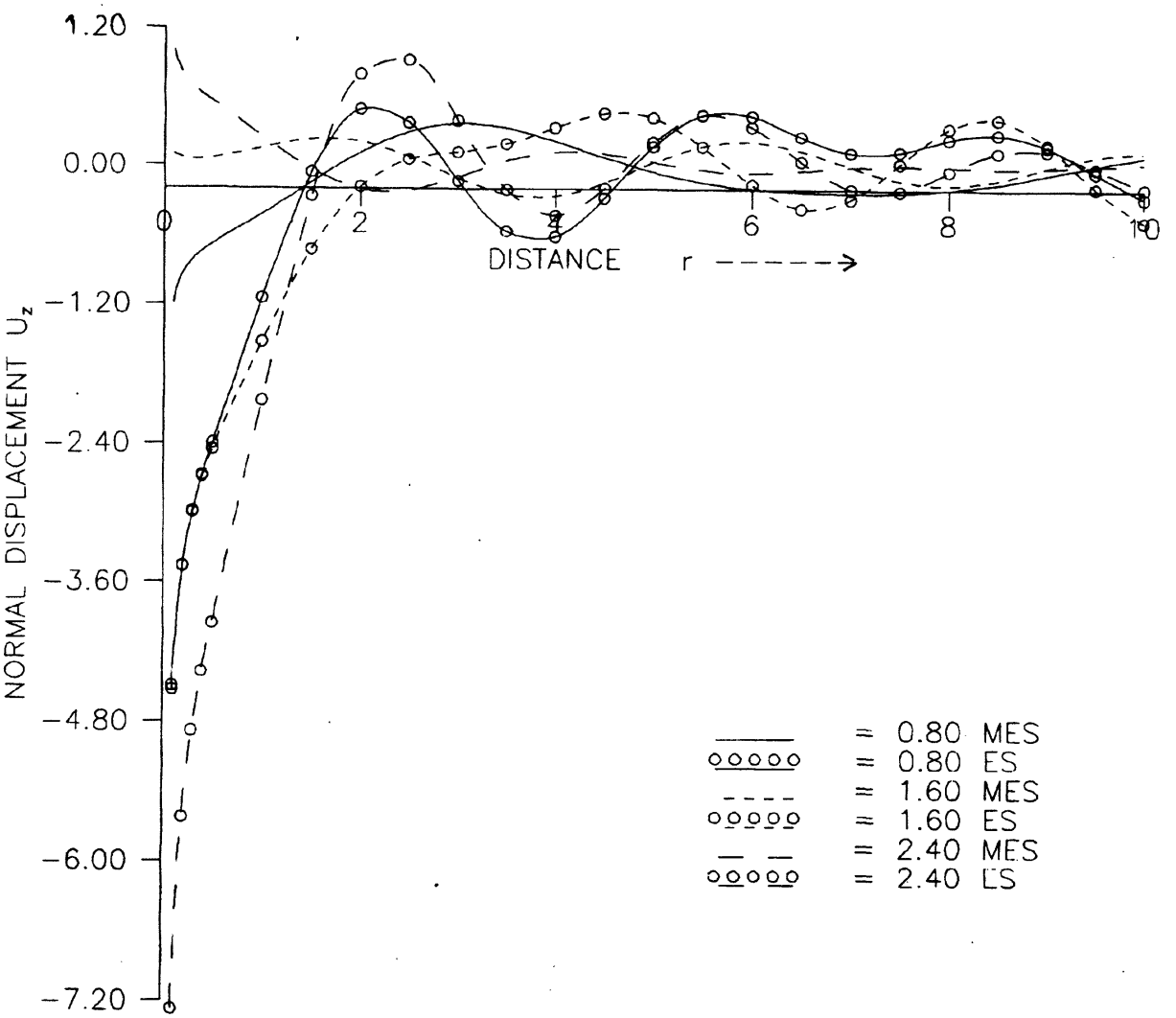

FIG. 1. Variations of normal displacement $U_z(= u_z/P)$ with distance r.

The behaviour of variations of T_{zz} for *MES* is opposite to that for *ES*. For *MES* the values of T_{zz} decrease sharply in the range $0 \le r \le 2$ and start oscillating in the further increase in value of r whereas for *ES* its values increase sharply in the range $0 \le r \le 2$ and then start oscillating just opposite to that for *MES*. For *MES*, initially, as the value of frequency increase its value decrease whereas for *ES* its behavior towards frequency is just opposite. The value of T_{zz} in *MES* have been magnified by multiplying its original value by 10 for all three frequencies in order to depict the comparison with *ES* theory and these variations have been shown in Fig. 2.

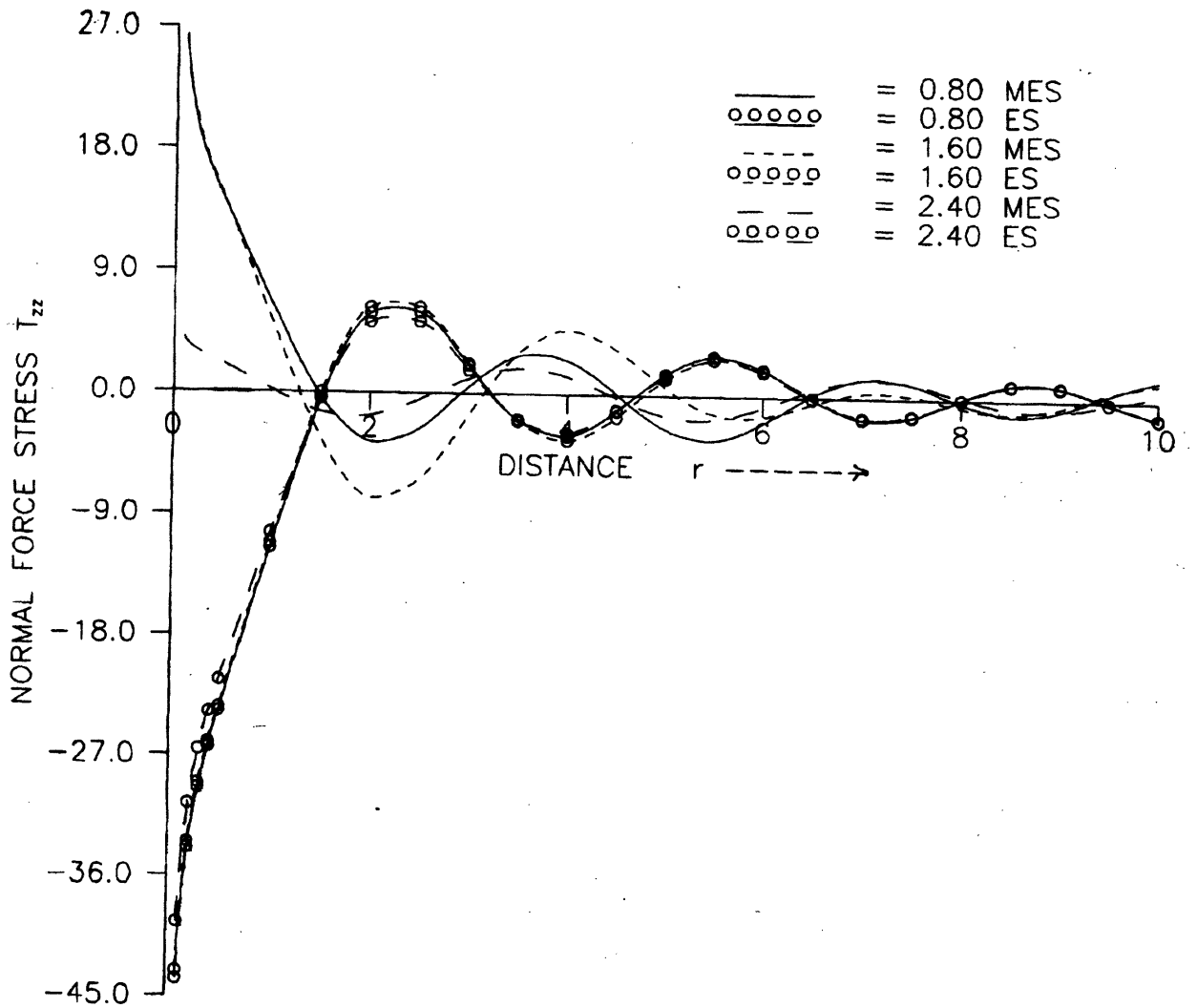

FIG. 2. Variations of normal force stress $T_{zz}(= t_{zz}/P)$ with distance r.

The variations of tangential couple stress $M_{z\theta}$ with distance 'r' for three different frequencies have been shown in Fig. 3. The behaviour of variations of $M_{z\theta}$ is same for all three frequencies whereas their corresponding values are different. For $\omega = 0.8$ and $\omega = 1.6$ the values of $M_{z\theta}$ increase sharply in the range $0 \leq r \leq 1.5$ and oscillate in the further range of r. For $\omega = 2.4$, its value initially is more than that for other two frequencies but its behaviour of variation is oscillating in the whole range of r.

Case II : Load in r-Direction

The variations of U_z, T_{zz} and $M_{z\theta}$ with distance 'r' when tangential point source is applied in radial direction have been shown in figs. 4, 5 and 6 respectively.

Fig. 4 shows the variations of normal displacement U_z with distance 'r'. The behaviour of variation of U_z is same for three different frequencies in both *MES* and *ES* theories while the corresponding values are slightly different. The values of U_z, for all the cases, decrease sharply in the range $0 \leq r \leq 2.5$ and start oscillating with the further increase in the value of r. For respective

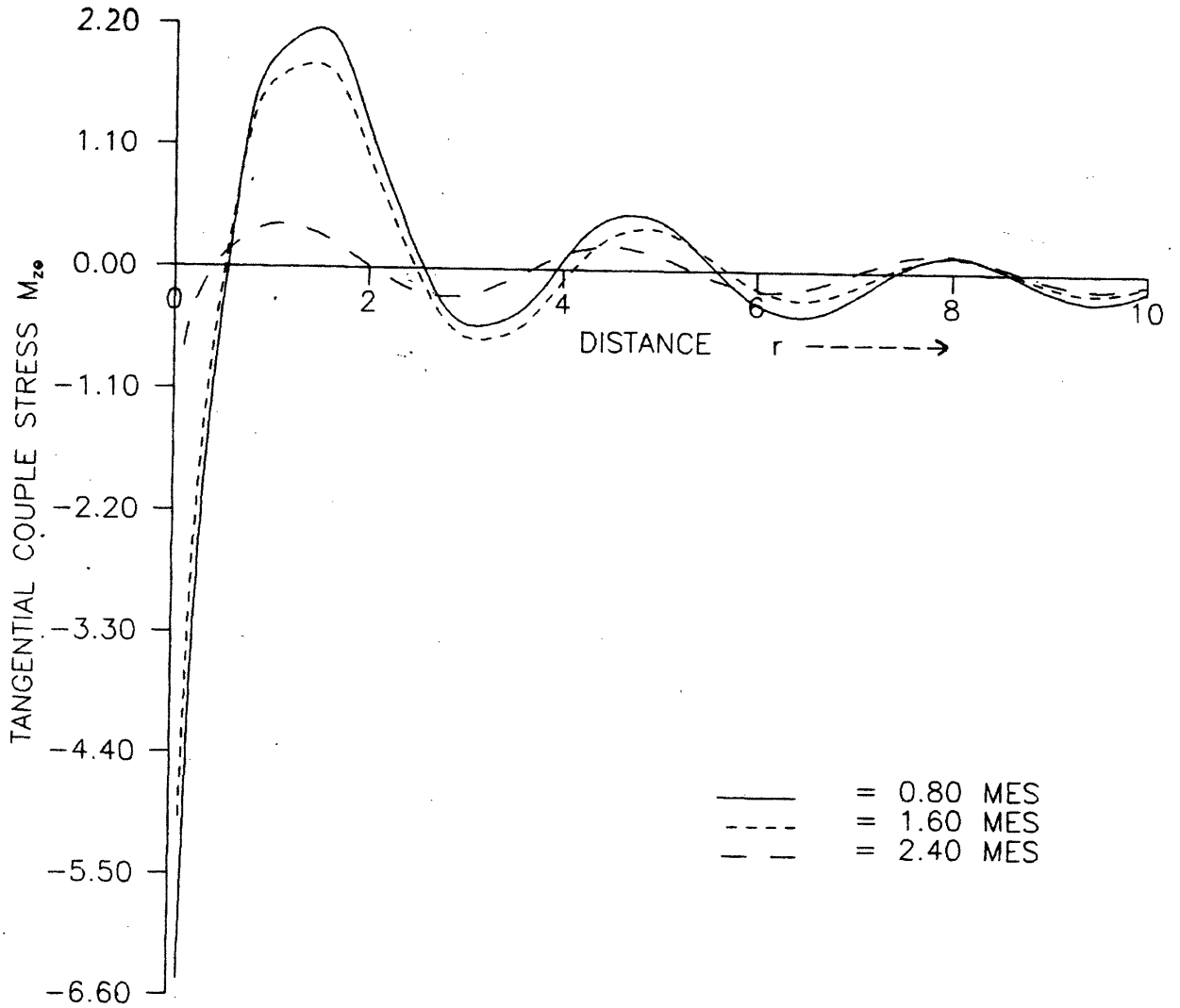

FIG. 3. Variations of tangential couple stress $M_{z\theta}(= m_{z\theta}/P)$ with distance r.

frequencies, its values for *MES* are less than that for *ES* in the range $0 \le r \le 2$. Initially, as frequency increases its value decrease for both *MES* and *ES*.

The variation of normal force stress T_{zz} with distance r have been shown in Fig. 5. For *ES*, the behaviour of variations of T_{zz} is same for three different frequencies while the corresponding values are slightly different. The values of T_{zz}, for *ES*, decrease sharply in the range $0 \le r \le 2$ and start oscillating with the further increase in value of r. For *MES* the behavior of variations is oscillating in whole the range for all the values of ω. For respective frequencies, its values for *MES* are less than that for *ES* in the range $0 \le r \le 2$. Initially, as frequency increases its value decrease for both *MES* and *ES*.

The behaviour of the variations of tangential couple stress $M_{z\theta}$ with distance 'r' have been shown in Fig. 6. The variations of $M_{z\theta}$ are same for frequencies $\omega = 0.80$ and $\omega = 1.60$, whereas their values are slightly different. For these frequencies the values of $M_{z\theta}$ increase sharply in the range $0 \le r \le 1.5$ then oscillate as r increase further. For $\omega = 2.4$ its value initially is more than that for other two frequencies but its behavior of variation is oscillating in the whole range.

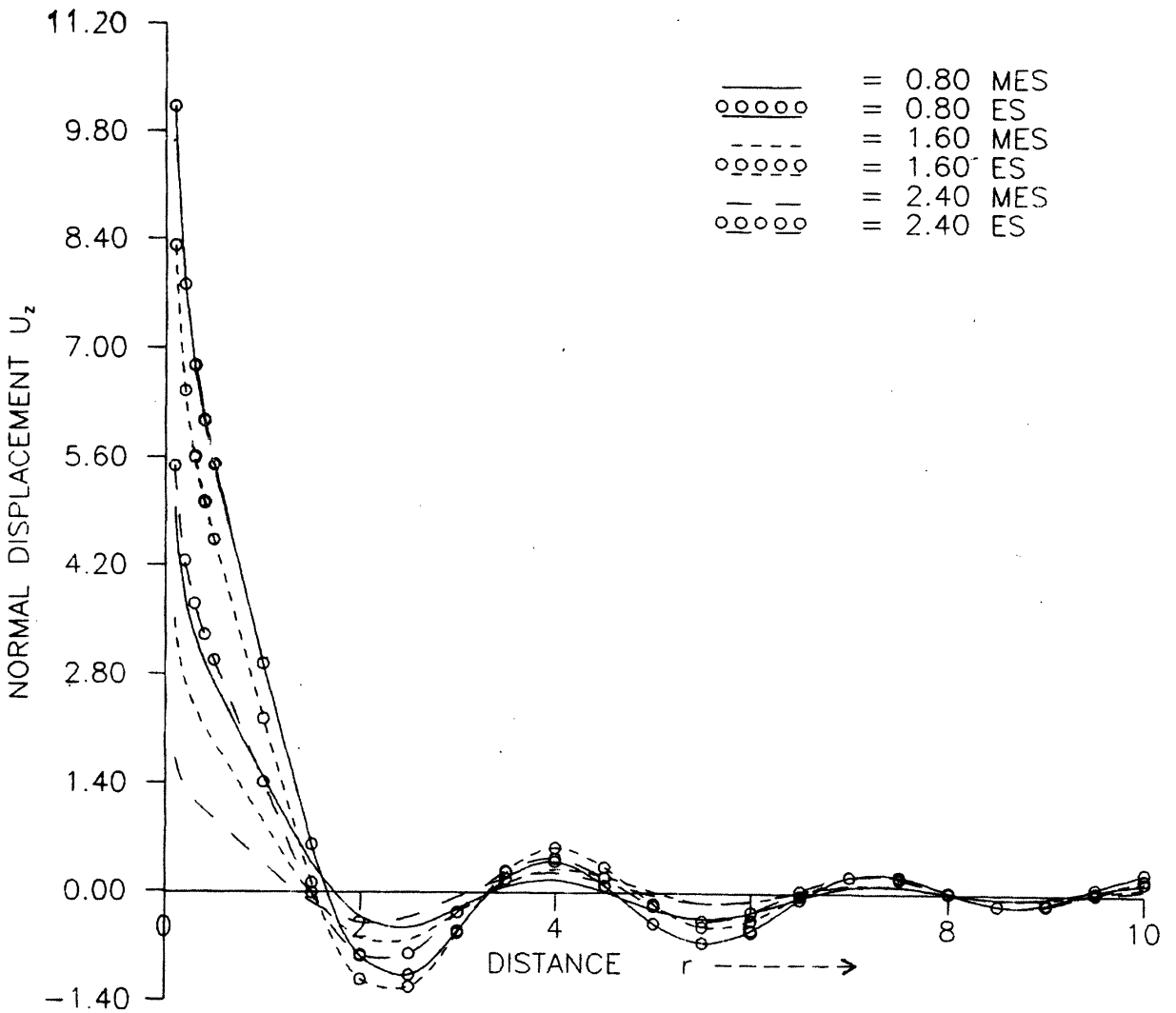

FIG. 4. Variations of normal displacement $U_z (= u_z/P)$ with distance r.

CONCLUSIONS

From the above numerical results, we conclude that micropolarity has a significant effect on normal displacement and normal force stress for all three dimensionless frequencies. Micropolarity effect is more appreciable very near to the point of application of source for both the case.

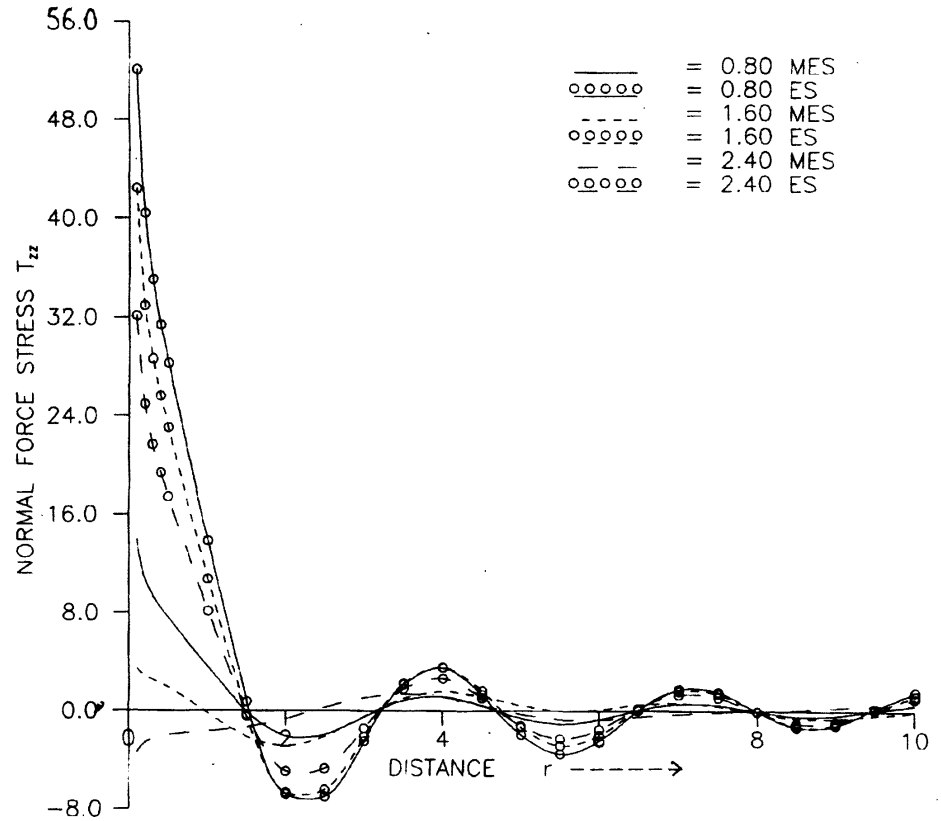

FIG. 5. Variations of normal force stress $T_{zz}(=t_{zz}/P)$ with distance r.

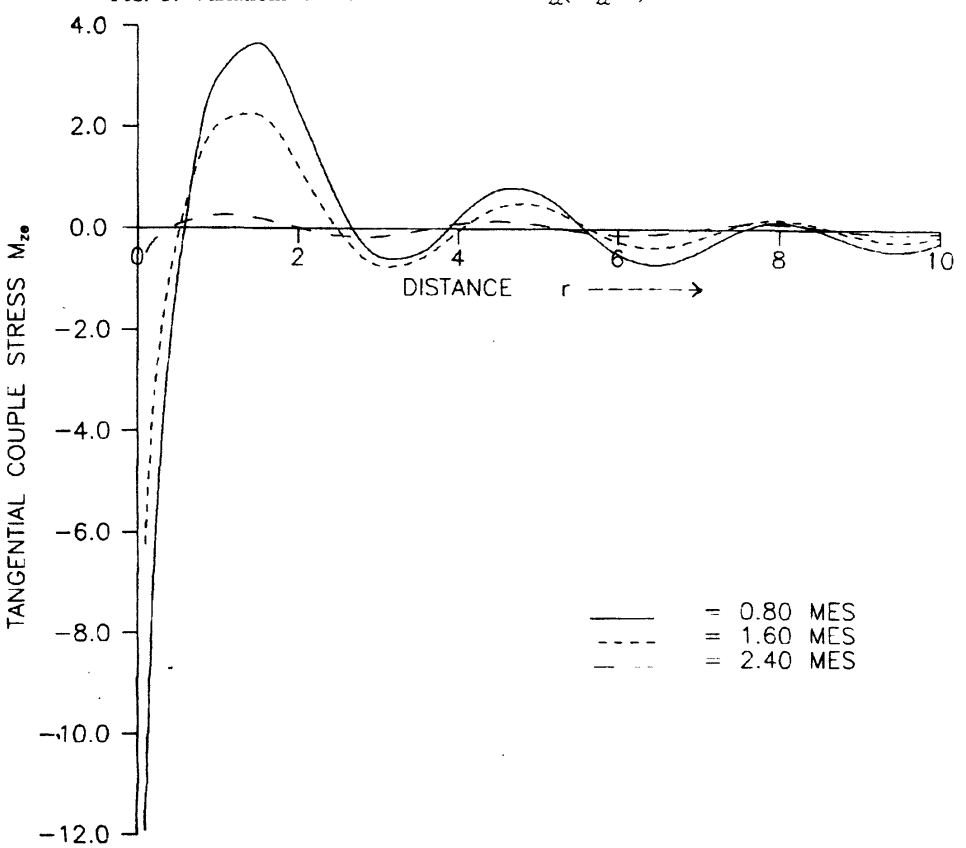

FIG. 6. Variations of tangential couple stress $M_{z\theta}(=m_{z\theta}/P)$ with distance r.

REFERENCES

1. Z. Q. Cheng and L. H. He, *Int. J. Engng. Sci.* **33** (1995) 389-97.
2. Z. Q. Cheng and L. H. He, *Int. J. Engng. Sci.*, **35** (1997) 659-68.
3. A. C. Eringen and E. S. Suhubi, *Int. J. Engng. Sci.*, **2** (1964) 189-203.
4. A. C. Eringen, *J. math. Mech.*, **15** (1966) 909-24.
5. A. C. Eringen, *Int. J. Engng. Sci.* **22** (1984) 1113-21.
6. R. Kumar and S. Deswal, *J. Sound Vibr.* **239** (2000) 467-88.
7. R. Kumar and S. Deswal, *Ganita*, **51** (2000) 187-206.
8. L. Nappa, *Int. J. Engng. Sci.*, **34** (1996) 1601-9.
9. W. H. Press, S. A. Tenkolsky, W. T. Vellerling and B. P. Flanner, *Numerical Recipes*, Cambridge University Press, Cambridge, 1986.
10. P. R. Sengupta and B. C. Ghosh, *Bull. Acad. Polon. Sci. Ser. Sci. Tech.*, **26** (1978) 455-65.
11. P. R. Sengupta and B. C. Ghosh, *Bull. Acad. Polon. Sci. Ser. Sci. Tech.*, **26** (1978) 467-80.
12. E. S. Suhubi and A. C. Eringen, *Int. J. Engng. Sci.*, **2** (1964) 389-404.
13. S. K. Tomar and R. Kumar, *Proc. Indian Acad. Sci. (Math. Sci)*, **109** (1999) 425-33.